The American Journal of Human Genetics, Volume *105*

Supplemental Data

CAKUT and Autonomic Dysfunction Caused by Acetylcholine Receptor Mutations

Nina Mann, Franziska Kause, Erik K. Henze, Anant Gharpure, Shirlee Shril, Dervla M. Connaughton, Makiko Nakayama, Verena Klämbt, Amar J. Majmundar, Chen-Han W. Wu, Caroline M. Kolvenbach, Rufeng Dai, Jing Chen, Amelie T. van der Ven, Hadas Ityel, Madeleine J. Tooley, Jameela A. Kari, Lucy Bownass, Sherif El Desoky, Elisa De Franco, Mohamed Shalaby, Velibor Tasic, Stuart B. Bauer, Richard S. Lee, Jonathan M. Beckel, Weiqun Yu, Shrikant M. Mane, Richard P. Lifton, Heiko Reutter, Sian Ellard, Ryan E. Hibbs, Toshimitsu Kawate, and Friedhelm Hildebrandt

Supplemental Appendix

SUPPLEMENTAL METHODS

Whole exome sequencing and homozygosity mapping. We obtained blood samples and pedigree information following informed consent from individuals with CAKUT. Approval for human subjects research was obtained from the Institutional Review Board at the respective institutions. Whole exome sequencing was performed as described previously using Agilent SureSelect™ human exome capture arrays (ThermoFisher) with next generation sequencing (NGS) on an Illumina™ platform (1). Sequence reads were mapped against the human reference genome (NCBI build 37/hg19) using CLC Genomics Workbench (version 6.5.1) (CLC bio). For homozygosity mapping, downstream processing of aligned BAM files were performed using Picard and samtools. SNV calling was done using GATK5 and the generated VCF file was subsequently used in homozygosity mapper. Genetic regions of homozygosity by descent were plotted across the genome as candidate regions for recessive genes as previously described (2). Mutation calling was performed in line with proposed guidelines by clinician-scientists who had knowledge of clinical phenotypes, pedigree structure, and genetic mapping (**Supplemental Figure 1**) (3). All variants were confirmed in original DNA using Sanger sequencing. The website GeneMatcher (https://genematcher.org/statistics) enabled the connection between researchers and providers caring for the families (4, 5).

cDNA cloning. Full length human *CHRNA3* (NM_000734.4) and *CHRNB4* (NM_000750.5) cDNAs were purchased from the Harvard PlasmID database (https://plasmid.med.harvard.edu). Human *CHRNA3* and *CHRNB4* (NM_000750.5) full-length cDNA and the two truncating variants, c.1010_1011delCA and c.1019C>G, were subcloned by PCR into the pENTR-D-TOPO vector (Thermo Fisher Scientific). Mutagenesis was performed using the QuikChange II XL site-directed mutagenesis kit (Agilent Technologies) to generate the c.267+2T>G and c.1010_1011delCA mutants. To represent the essential splice site mutation, c.267+2T>G, which is predicted to lead to in-frame skipping of exon 3, we generated a cDNA construct with exon 3 deleted. Primers used for subcloning and mutagenesis are listed in **Supplementary Table S1**. Expression vectors were generated using LR clonase (Thermo Fisher Scientific) following the manufacturer's instruction. The expression vector pcDNA6.2-C-GFP (Thermo Fisher Scientific) was used in this publication.

Cell culture and transient transfections. Experiments were performed in HEK293 cells purchased from the American Type Culture Collection (ATCC) biological resource center. For transient transfections, HEK293 cells were seeded at 40-50% confluency in DMEM, supplemented with 10% fetal calf serum and 1% penicillin/streptomycin and grown overnight. Transfections were carried out using Lipofectamine2000 (Thermo Fisher Scientific) and OptiMEM (Thermo Fisher Scientific) following the manufacturer's instructions. Cell lines were tested monthly for mycoplasma contamination.

Immunofluorescence and confocal microscopy in cell lines. For immunostaining, HEK293 cells were seeded on Fibronectin-coated coverslips in 6-well plates. After 24 hours, cells were transiently transfected with 800-1000ng of DNA using Lipofectamine2000 (Thermo Fisher Scientific) following the manufacturer's instructions. Experiments were performed 24–48 hours after transfection. Cells were fixed for 10 minutes using 2% paraformaldehyde at room temperature. If permeabilization was done, cells were incubated for 10 minutes in 0.5% Triton X-100. For immunostaining of unpermeabilized cells, this permeabilization step was skipped. Cells were then blocked with 10% donkey serum + 1% BSA and incubated with primary antibody overnight at 4°C. The following day, cells were incubated in secondary antibody for 60 minutes at room temperature, and subsequently stained for 5 minutes with 4',6-diamidino-2-phenylindole (DAPI) in PBS. Confocal imaging was performed using the Leica SP5X system with an upright DM6000 microscope, and images were processed with the Leica AF software suite. Immunofluorescence experiments were repeated at least three times in independent experiments. The following antibodies were used for immunofluorescence experiments with similar results: rabbit anti-CHRNA3 (SAB2104205, Sigma), diluted 1:100 and rabbit anti-CHRNA3 (NBP2-30060, Novus), diluted 1:100. Donkey anti-rabbit secondary antibody conjugated to Alexa Fluor 594 was purchased from Invitrogen.

Whole cell electrophysiology in HEK293 cells. All chemicals were purchased from Sigma-Aldrich unless otherwise noted. HEK293 cells used for electrophysiology experiments were purchased from ATCC and were used from passages 5-30. Cells were maintained in DMEM (Gibco) supplemented with 10% FBS (Atlanta Biologicals) and 10 ug/ml gentamicin (Gibco). Two days prior to recording, HEK293 cells were plated at low density onto 12 mm glass coverslips (VWR) in wells of a 6-well plate (Greiner). Cells were transfected with 300-700 ng DNA after 24 hours using FuGENE6 (Promega) according to the manufacturer's instructions. Whole cell electrophysiological recordings were carried out 16-24 hours after transfection. Borosilicate glass pipettes (Harvard Apparatus) were pulled and heat polished to a final resistance of 2-4 MΩ and backfilled with (in mM) 147 NaCl, 10 EGTA, and 10 HEPES (adjusted to pH 7.0 with NaOH). Patches were obtained in an external buffer containing (in mM) 147 NaCl, 2 KCl, 2 $CaCl_2$, 1 $MgCl_2$, 13 glucose, 10 HEPES (adjusted to pH 7.3 with NaOH), then perfused with acetylcholine (ACh) using a rapid solution exchange system (RSC-200; Bio-Logic). Currents were recorded using an Axopatch 200B patch clamp amplifier (Axon Instruments), filtered at 2 kHz (Frequency Devices), digitized with a Digidata 1440A (Axon Instruments) with a sampling frequency of 10 kHz, and analyzed using the pCLAMP 10.5 software (Axon Instruments).

Table S1: Primer sequences used for subcloning and mutagenesis.

Human *CHRNA3* pENTR cloning primer sequences		
Target	Forward Primer (5'-3')*	Reverse Primer (5'-3')
Wild Type	CACCATGGGCTCTGGCCCGCTC	TGCATCTTCCCTGGCC
Thr337Asnfs*81	CACCATGGGCTCTGGCCCGCTC	GCACTGAAATTGGAGATTTTTATCC
Ser340*	CACCATGGGCTCTGGCCCGCTC	GGGCATTGTGTGTGTCGTC
Human *CHRNA3* mutagenesis primer sequences		
Target	Forward Primer (5'-3')	Reverse Primer (5'-3')
Essential Splice (Exon 3 skipping)	TCTCAGCTGGTGAAGGTGATCTGGAATG ACTACAAG	CTTGTAGTCATTCCAGATCACCTTCACCA GCTGAGA
Thr337Asnfs*81	CCCGACGACACACAATGCCCTCATGGGT	ACCCATGAGGGCATTGTGTGTCGTCGGG
Human *CHRNB4* pENTR cloning primer sequences		
Target	Forward Primer (5'-3')	Reverse Primer (5'-3')
Wild Type	CACCATGAGGCGCGCGCCTTCCC	CTAGTCACGCTGGGCAGCGTAG

*The underlined CACC in the forward primer provides part of the Kozak consensus sequence and allows for directional cloning

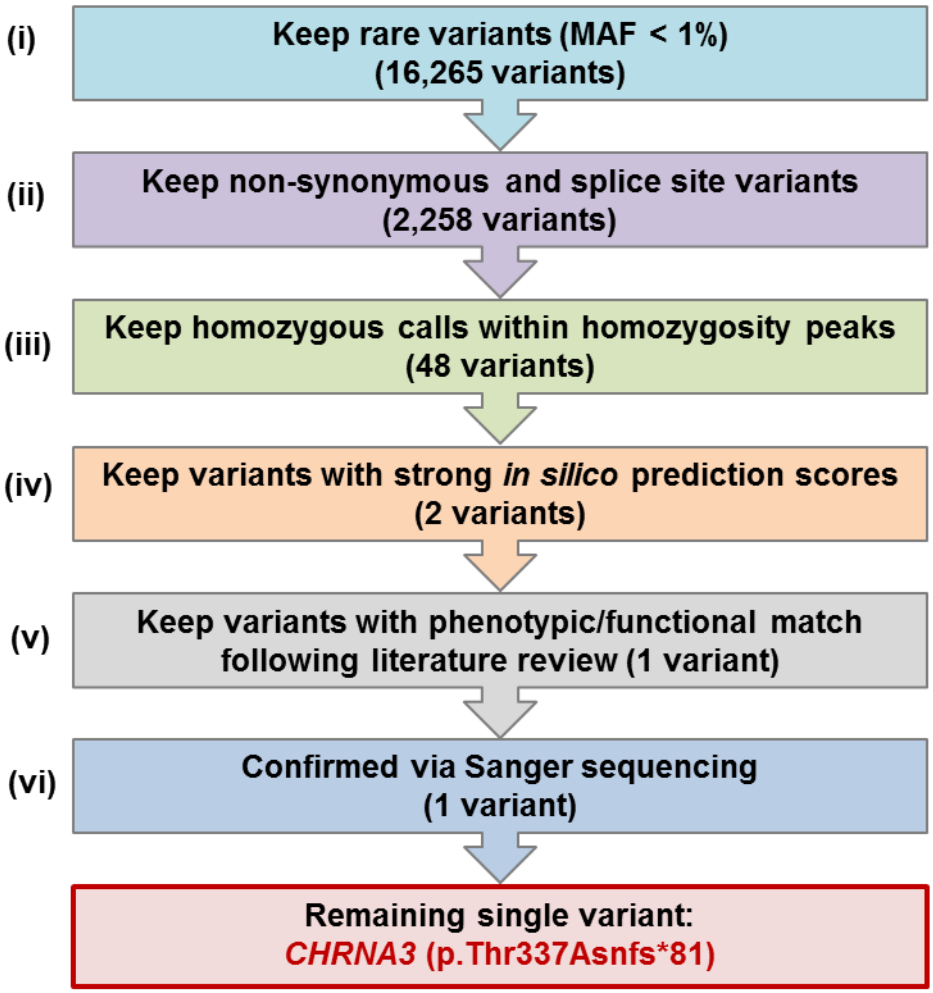

Figure S1. Variant filtering process from whole exome sequencing data for the proband from the index family, B1717-21.

i) Keep rare variants that are present with a minor allele frequency (MAF) <1% in healthy control cohorts (NHLBI Exome Sequencing Project, Exome Aggregation Consortium, Genome Aggregation Database, 1000 Genomes Project).

ii) Keep non-synonymous variants and intronic variants that are located within splice sites.

iii) Due to presence of consanguinity, apply an autosomal recessive hypothesis and overlap surviving variants with the homozygosity mapping. Keep all homozygous calls within the regions of homozygosity by descent.

iv) Rank remaining variants based on their predicted likelihoods of being deleterious for the function of the encoded protein. Keep variants that are protein-truncating (i.e. nonsense, frameshift, obligatory splice, or loss of start or stop codons) or that are highly conserved across phylogeny and predicted to be deleterious based on at least two of three prediction programs (PoyPhen2, SIFT, and MutationTaster).

v) Review literature on remaining variants, and keep variants with known role in the kidney or bladder, or with animal models that match the patient phenotype.

vi) Sanger confirm variant in original DNA.

The only remaining variant following this process was a homozygous truncating mutation in *CHRNA3* (Thr337Asnfs*81).

A Renal and Bladder Imaging for B1402

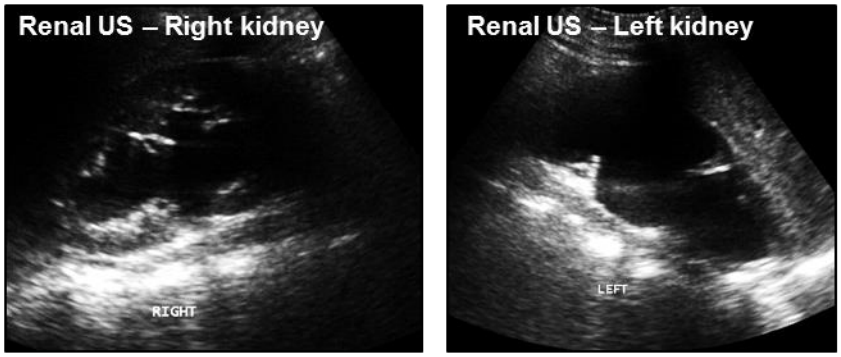

B Renal and Bladder Imaging for B1717-21

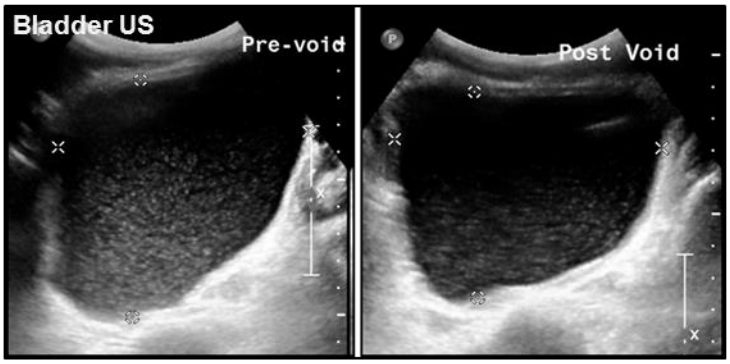

C Renal and Bladder Imaging for GM-21

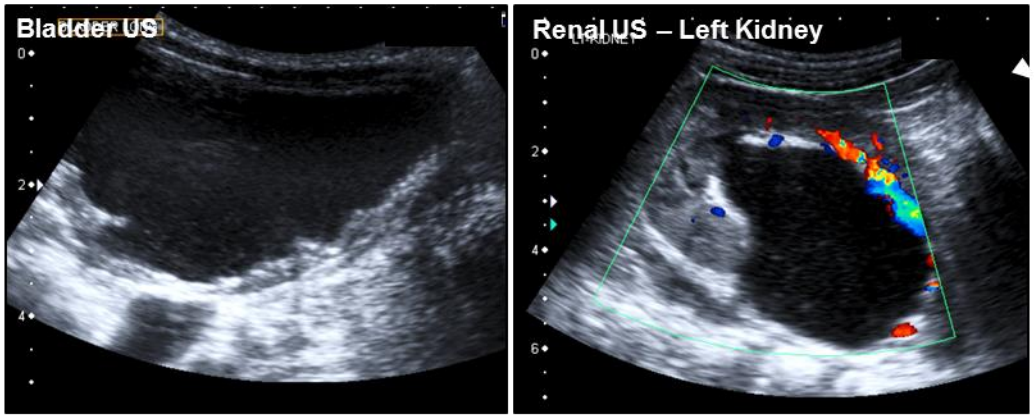

Figure S2. Additional renal and bladder imaging.

(A) Imaging for individual B1402. Renal ultrasounds depicting bilateral hydronephrosis.

(B) Imaging for individual B1717-21. Pre- and post-void ultrasound imaging of the bladder depict poor bladder emptying with a large post-void residual.

(C) Imaging for individual GM-21. Bladder ultrasound (left image) depicts a thickened, trabeculated bladder wall, while renal ultrasound (right image) demonstrates marked hydronephrosis and cortical thinning.

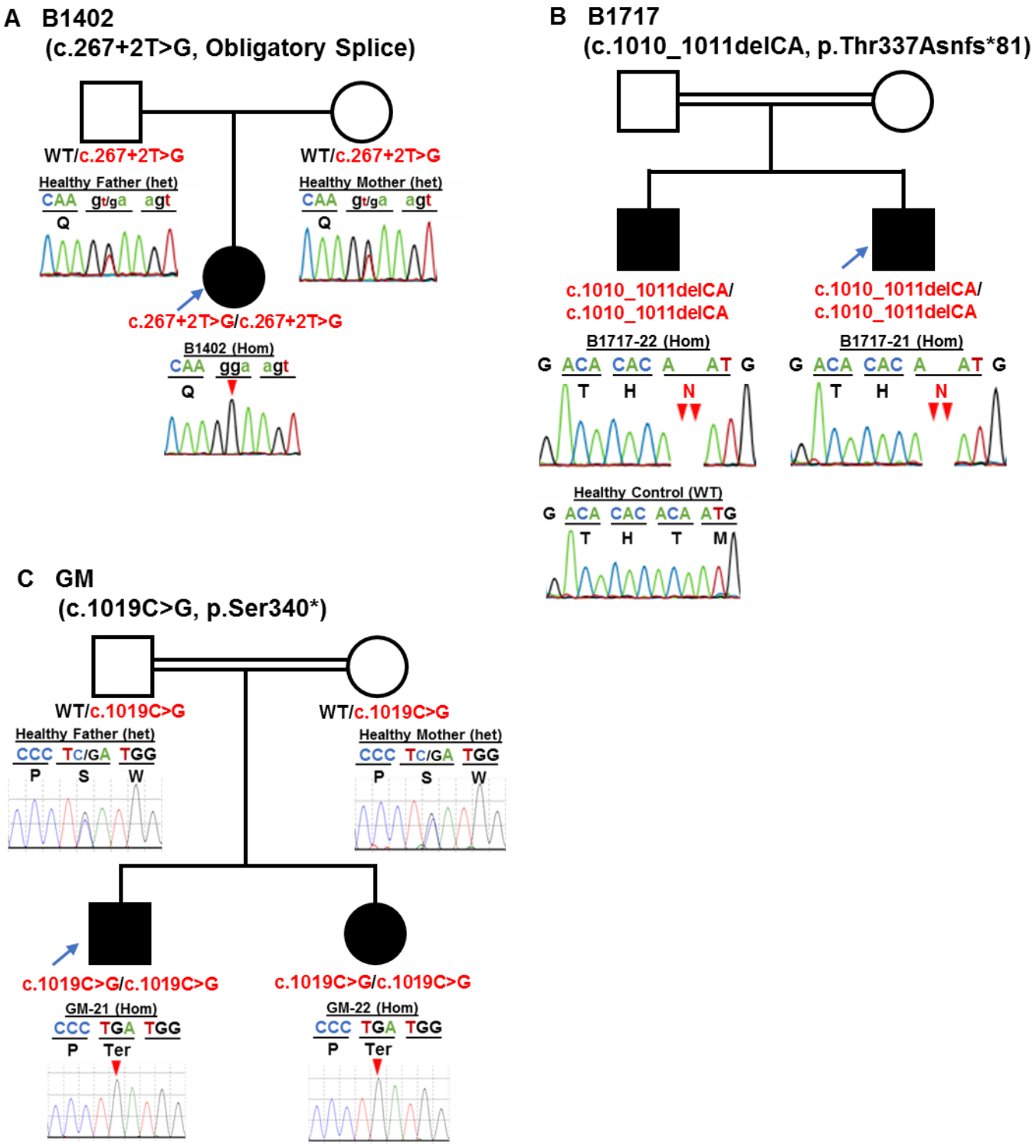

Figure S3. Sanger sequencing for three families with mutations in *CHRNA3*.

The pedigrees and Sanger tracings for the three families (**A-C**) in whom mutations in *CHRNA3* were identified are depicted here. In the pedigrees, squares represent males and circles represent females. Open symbols represent unaffected individuals, and filled symbols represent affected individuals. Consanguineous unions are depicted as double horizontal lines. Individual genotypes from Sanger sequencing are shown. Probands are denoted by blue arrows.

het, heterozygous; Hom, homozygous; Ter, termination; WT, wild type

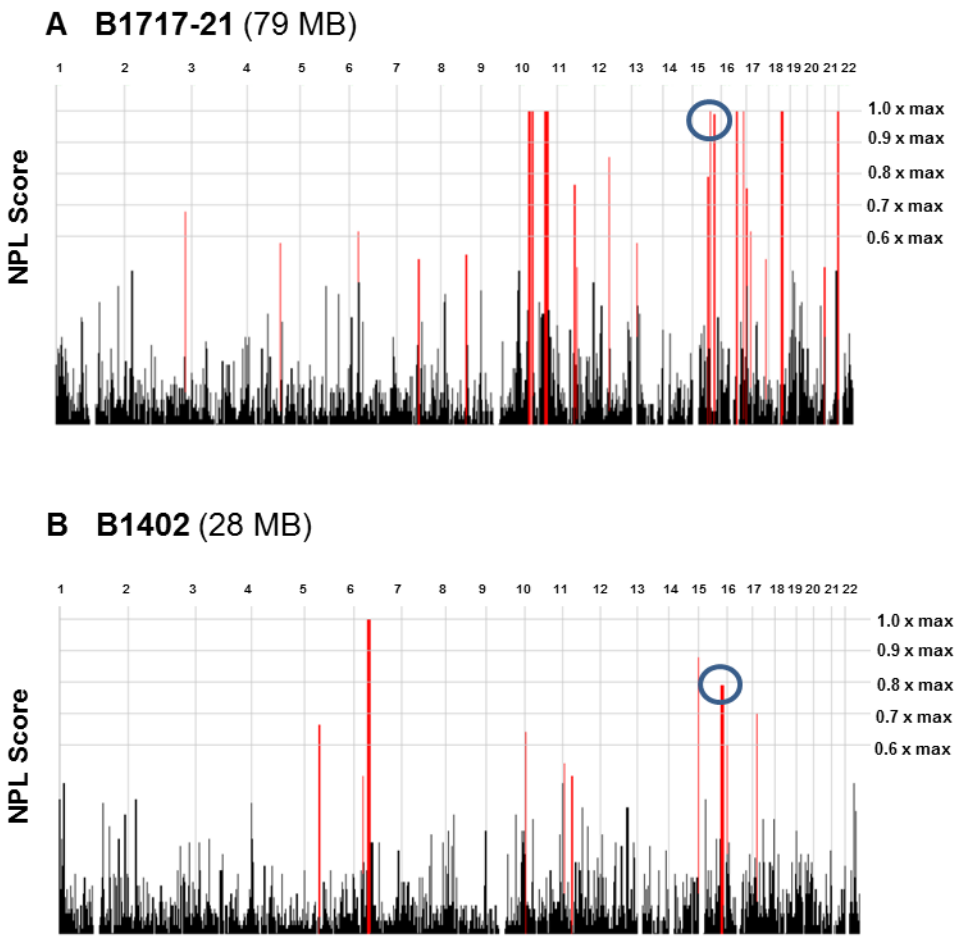

Figure S4. Homozygosity mapping for affected individual B1717-21 and B1402.

Homozygosity mapping for two affected individuals, B1717-21 and B1402, is depicted here. Chromosomal position is aligned along the X-axis. Peaks (red) indicate regions of homozygosity by descent. Both probands have a peak on chromosome 15 where *CHRNA3* is located. The megabases (MB) of homozygosity for each patient is indicated in the figure captions.

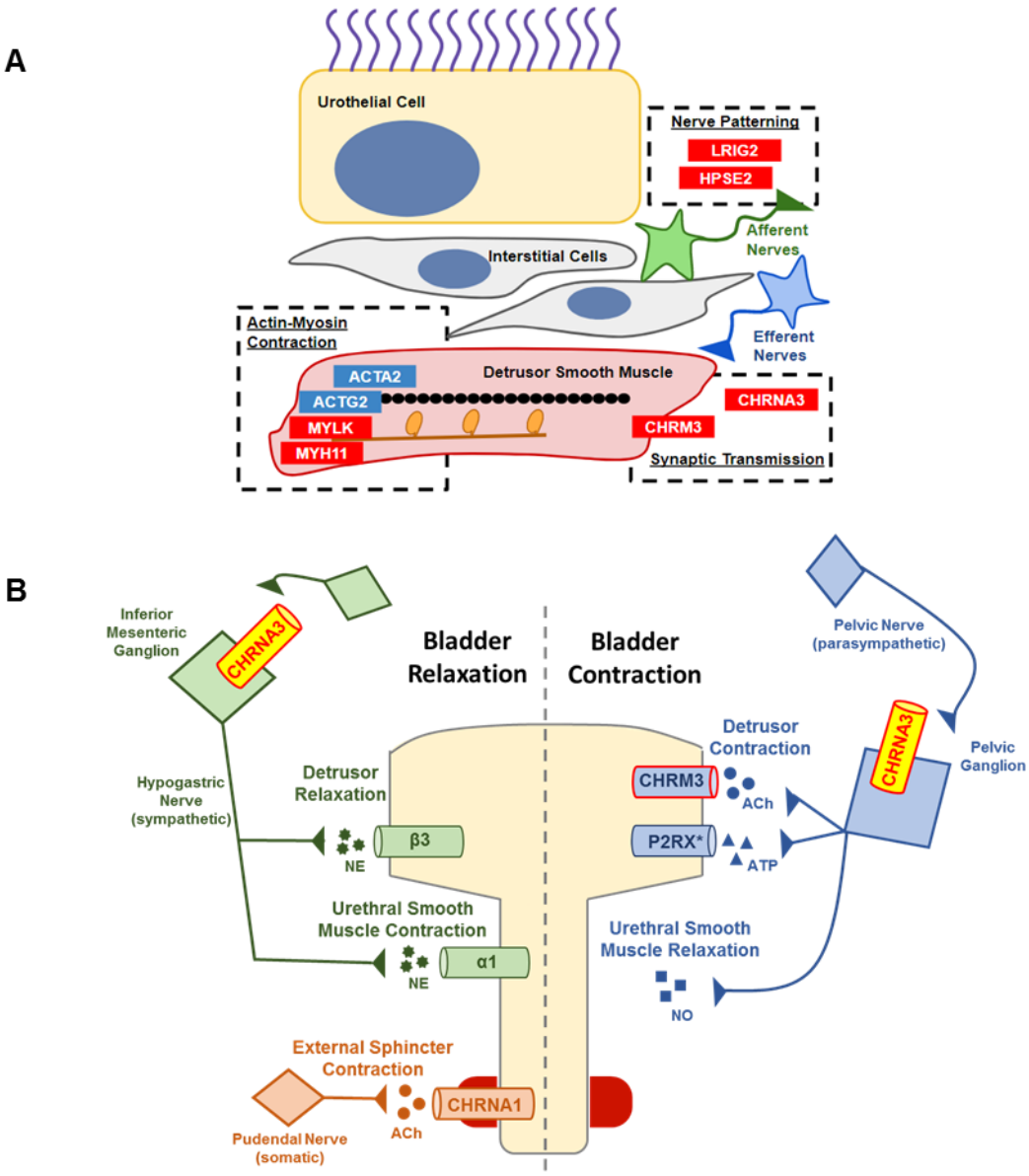

Figure S5. Monogenic causes of bladder dysfunction.

(A) Schematic of monogenic causes of bladder dysfunction. This includes mutations in genes that disrupt actin-myosin contraction of the detrusor smooth muscle *(ACTA2, ACTG2*, *MYLK*, *MYH11*), genes that disrupt neuronal patterning (*LRIG2*, *HPSE2*), as well as genes that affect neuronal synaptic transmission (*CHRNA3*, *CHRM3*). Genes in red are inherited in an autosomal recessive fashion, while those in blue are inherited in an autosomal dominant manner.

(B) Schematic diagram depicting the neuronal innervation to the bladder and the role of *CHRNA3* in regulating bladder and urethral relaxation and contraction. *CHRNA3* is expressed in both the sympathetic (green) and parasympathetic (blue) ganglia. The sympathetic nervous system mediates bladder relaxation. The post-ganglionic hypogastric nerve stimulates β3 and α1 adrenergic receptors to mediate detrusor relaxation and urethral smooth muscle contraction, respectively. The parasympathetic nervous system is activated during voiding, and mediates detrusor contraction via muscarinic acetylcholine receptors (*CHRM3*) and purinergic receptors (*P2RX**). It also mediates urethral smooth muscle relaxation via nitrous oxide signaling. Muscle-type nicotinic acetylcholine receptors also facilitate contraction of the external urethral sphincter (orange). The receptors encoded by genes that, if mutated, cause monogenic forms of CAKUT (*CHRM3*, *CHRNA3*) are outlined in red.

Adapted from Fowler et al., *Nature Reviews Neuroscience*, 9:452, 2008.

REFERENCES

1. Braun DA, Lovric S, Schapiro D, Schneider R, Marquez J, Asif M, Hussain MS, Daga A, Widmeier E, Rao J, et al. Mutations in multiple components of the nuclear pore complex cause nephrotic syndrome. *The Journal of clinical investigation.* 2018;128(10):4313-28.
2. Hildebrandt F, Heeringa SF, Ruschendorf F, Attanasio M, Nurnberg G, Becker C, Seelow D, Huebner N, Chernin G, Vlangos CN, et al. A systematic approach to mapping recessive disease genes in individuals from outbred populations. *PLoS genetics.* 2009;5(1):e1000353.
3. MacArthur DG, Manolio TA, Dimmock DP, Rehm HL, Shendure J, Abecasis GR, Adams DR, Altman RB, Antonarakis SE, Ashley EA, et al. Guidelines for investigating causality of sequence variants in human disease. *Nature.* 2014;508(7497):469-76.
4. Sobreira N, Schiettecatte F, Valle D, and Hamosh A. GeneMatcher: a matching tool for connecting investigators with an interest in the same gene. *Human mutation.* 2015;36(10):928-30.
5. Sobreira N, Schiettecatte F, Boehm C, Valle D, and Hamosh A. New tools for Mendelian disease gene identification: PhenoDB variant analysis module; and GeneMatcher, a web-based tool for linking investigators with an interest in the same gene. *Human mutation.* 2015;36(4):425-31.